New Spirit of an Old Technique: Characterization of Lipid Phase Transitions via UV/Vis Spectroscopy

Petra Maleš[a], Zlatko Brkljača[a], Darija Domazet Jurašin[b], Danijela Bakarić[a, *]

[a] Division for Organic Chemistry and Biochemistry, Ruđer Bošković Institute, Bijenička 54, 10000 Zagreb, Croatia

[b] Division for Physical Chemistry, Ruđer Bošković Institute, Bijenička 54, 10000 Zagreb, Croatia

Abstract:

One of the advantages of investigating lipid phase transitions by thermoanalytical techniques such as DSC is manifested in the proportionality of the signal strength on a DSC curve, attributed to a particular thermotropic event, and its cooperativity degree. Accordingly, the pretransition of 1,2-dipalmitoyl-s*n*-glycero-3-phosphocholine (DPPC) is less noticeable than its main phase transition; as a matter of fact, when DSC measurements are performed at low heating rate, such low-cooperativity phase transition could go (almost) unnoticed. The aim of this work is to present temperature-dependent UV/Vis spectroscopy, based on a temperature-dependent change in DPPC suspension turbidity, as a technique applicable for determination of lipid phase transition temperatures. Multivariate analyzes of the acquired UV/Vis spectra show that phase transitions of the low-cooperativity degree, such as pretransitions, can be identified with the same certainty as transitions of a high-cooperativity degree.

Keywords:

UV/Vis spectroscopy, 1,2-dipalmitoyl-*sn*-glycero-3-phosphocholine (DPPC), cholesterol, lipid phase transitions, differential spectral analysis (DSA), multivariate curve analysis (MCA)

1. Introduction

Uni- and multilamellar liposomes as well as supported lipid bilayers constituted from 1,2-dipalmitoyl-s*n*-glycero-3-phosphocholine (DPPC, Fig. 1) are frequently utilized as model lipid membranes [1,2]. Although DPPC is far from being representative phosphocholine in biological

membranes, the most important reason for its intensive use lies in the fact that the transition of DPPC from gel ($L_{\beta'}$) to fluid phase (L_{α}) (main phase transition) displays a peak at $T_m \approx 41$ °C [3], making the latter easily accessible by the vast majority of experimental techniques. This advantage is reflected in the possibility to unravel the mechanism of water permeation across the bilayer; as the latter reaches maximum at T_m in lipid membranes [4–7], DPPC serves as suitable model system in assessing the structural transitions and dynamics allowing water to translocate across the membrane [8–10]. The experimental elucidation of the pattern and site of incorporation of potential drugs in DPPC lipid bilayers [11–16] is usually achieved via the temperature-dependent behavior of the latter; since the signals originated from different lipid parts (phosphate, choline, glycerol backbone, hydrocarbon chains) vary differently in the absence/presence of drugs, with the maximum difference at T_m, the reconstruction of the incorporation of drugs into the DPPC bilayer becomes indirectly enabled. In spite of the reported benefits, the utility of DPPC as model lipid lacks in certain aspects: first, when studying the interaction of drug and model lipid membrane significantly higher drug concentrations are required compared to the physiological ones in order to induce lipid signal changes, which in turn affects their mutual interactions [17]; second, at physiological temperature (37 °C) DPPC is found in a ripple phase ($P_{\beta'}$), the appearance of which is generally exceptionally sensitive on the additive presence in DPPC bilayer [18,19]. At the same time the latter opens the possibility that subtle changes in $P_{\beta'}$ properties, caused by the incorporation of a much smaller amount of drugs, could indirectly provide insight into drug location and interaction pattern. In turn, discussed disadvantages could be reduced by applying a technique sensitive enough to record the signals of both lipid and incorporated compound even at low concentrations, and, at the same time, be able to identify $P_{\beta'}$ and the associated changes.

As much as the manipulation of drug (or any other additive) concentration is trivial, so much is the characterization of $P_{\beta'}$ complicated. Although the geometrical and dynamical properties of periodic undulations observed on the DPPC surface have been described by different structural [20–29], microscopic [22,30], spectroscopic [31–36] and computational [37–41] techniques, there are still disagreements in explaining their origin; according to one hypothesis, all DPPC lipids are found in gel phase (see, for example, [31] and references therein), whereas another one supports the coexistence of DPPC lipids in gel ($L_{\beta'}$) and fluid (L_{α}) domains [42]. Nevertheless, a crucial role of cooperativity for undulations detection [43] is substantiated by the exceptional sensitivity of $L_{\beta'} \rightarrow P_{\beta'}$ transition to the lamellarity of the investigated lipid

membranes [3,19,44], as well as to the medium in which the membranes are suspended [45–48].

The aim of this paper is to lay the basis for the development of a technique that could simultaneously record the signals of liposome-incorporated drug at low concentrations, and detect the occurrence and/or change in $P_{\beta'}$ phase. The former criterion might be met by temperature-dependent UV/Vis spectroscopy since it is one of the simplest and most routinely used techniques in exploration of liposome-incorporated drugs release when the latter possess chromophore(s) that absorb in UV/Vis spectral range [49–51]. Further advantage associated with utility of temperature-dependent UV/Vis spectroscopy is the ability to identify the corresponding signals even at very low concentrations and, due to UV/Vis transparency of drug-free liposome suspensions, the discrimination of drug-incorporated and drug-released signals is facilitated. The lack of UV/Vis signatures of pure DPPC liposome suspensions is a crucial reason why this technique was rarely applied in determination of DPPC phase transition temperatures [52–54]. For instance, by measuring the temperature dependence of the absorbance of the signal at 400 nm, which was formed as a result of turbidity of the solution, Cevc *et al.* managed to determine main phase transition temperature of membranes under exploration [55]. However, multivariate techniques such as multivariate curve analysis with alternating least squares and evolving factor analysis (MCR-ALS/EFA) [31] might be powerful enough to detect temperatures of phase transitions of lower cooperativity such as pretransition. With this in mind this, we decided to explore suspension of multilamellar DPPC liposomes in aqueous solution of NaCl (I(NaCl) = 100 mM) via DSC (as a reference technique) and temperature-dependent UV/Vis spectroscopy; furthermore, multivariate techniques were employed on the latter in order to assess its potential in determination of DPPC pre- and main phase transition temperatures. A suspension of DPPC and cholesterol (CHOL; Fig. 1), with mole fraction of CHOL being x(CHOL) ≈ 20 %, and saturated aqueous CHOL solution were used as reference systems in which, in the examined temperature range, the pretransition or any phase transition, respectively, is not expected [56,57]. Since phase transition temperatures of lipid membranes can be modulated by the change in the ionic strength and the content of the hydrating medium [45–48,58–60], DPPC liposomes (in the absence of CHOL) were prepared in two additional hydrating media and these data are presented in Supporting Information.

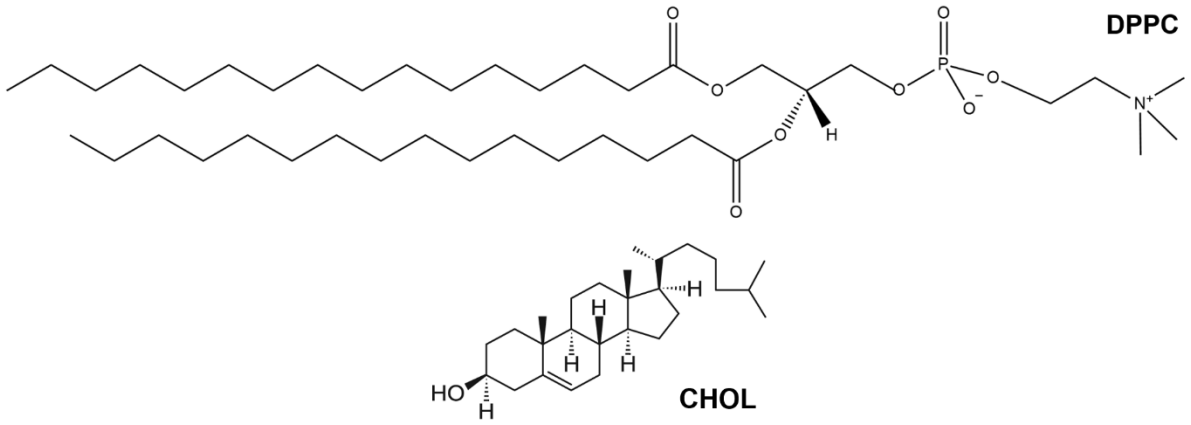

Fig. 1. Structural formula of 1,2-dipalmitoyl-*sn*-glycero-3-phosphocholine (DPPC) and cholesterol (CHOL).

2. Experimental

2.1 Chemicals and multilamellar liposomes preparation

1,2-Dipalmitoyl-*sn*-glycero-3-phosphocholine (DPPC; white powder, ≥ 99 %) and cholesterol (CHOL; white powder, 98 %), purchased from Avanti Polar Lipids, were dissolved in chloroform ($CHCl_3$; colorless liquid, p.a., Carlo Erba) to give a stock solutions of concentration of γ(DPPC) =10 mg ml^{-1} and γ(CHOL) = 1 mg ml^{-1}. The latter were further used in the preparation of DPPC and DPPC + 20% CHOL films intended for the preparation of multilamellar DPPC and DPPC + 20% CHOL liposomes, respectively, for DSC and UV/Vis measurements. After pipetting the appropriate amount of DPPC (and/or CHOL) stock solution into each flask (DPPC: 2 ml of DPPC stock solution for DSC and 1 ml for UV/Vis measurements, respectively; DPPC + 20% CHOL: 5 ml of DPPC stock solution and 4.65 ml of CHOL stock solution for DSC and 1 ml of DPPC stock solution and 0.950 ml of CHOL stock solution for UV/Vis measurements, respectively; CHOL: 2 ml of CHOL stock solution for DSC and 1 ml for UV/Vis measurements, respectively), $CHCl_3$ was evaporated on a rotary evaporator in order to get DPPC, DPPC + 20% CHOL and CHOL films, respectively. Following their drying under an Ar stream the films in the flasks intended for DSC and UV/Vis measurements were suspended in 4 ml and 10 ml, respectively, with aqueous (milli-Q water) solution of NaCl (Kemika, p. a. grade) with ionic strengths I = 100 mM (pH ≈ 6.5). DPPC liposomes (in the absence of CHOL) were additionally prepared in aqueous solution of NaCl of higher ionic strength (I(NaCl) = 400 mM), and in phosphate buffer (PB) (composed from sodium hydrogen phosphate (Na_2HPO_4, Alfa Aesar, > 99%) and sodium dihydrogen phosphate

(NaH_2PO_4, Fluka, p.a.)) of the same ionic strength as the reference solution (I = 100 mM) but of different chemical composition and pH (pH = 7.1) (these data are displayed in Supporting Information). Suspended films were vortexed, retained in a hot H_2O bath (heated up to 70 °C) and cooled in an ice bath following the Bangham's procedure [61]. The samples were held for 2 minutes during each step, with the whole procedure performed in three to five cycles. The final mass concentrations of lipids for DSC and UV/Vis measurements were γ = 5 mg ml^{-1} and γ = 1 mg ml^{-1}, respectively (in pure CHOL saturated solution was further examined). All chemicals were used as received.

2.2 UV/Vis spectroscopy: Temperature-dependent spectral acquisition, data preparation and spectral analysis of hydrated multilamellar liposomes

UV/Vis spectra were measured on UV/Vis spectrophotometer NanoDrop Thermo Scientific Nanodrop 2000 (Thermo Fisher Scientific, USA) in the spectral range 250 − 500 nm. Sealed quartz cuvettes (sample volume 1 ml) were placed in a temperature-controlled cuvette holder and heated in a temperature interval of 30 − 52 °C. Every sample was recorded three times (in three different cuvettes) except for the aqueous solution(s) of NaCl (and PB) which were recorded once.

After smoothing the acquired spectra (Savitzky-Golay; polynom of a 3rd degree and 10 points) [62], further analyses were undertaken on the prepared UV/Vis spectra in the range 250 − 300 nm, as this range possesses the greatest sensitivity on sample turbidity change. The latter is manifested as the shift in the background signal absorbance, whose variations coincide with temperature-dependent behavior of DPPC multilamellar liposomes (Fig. 2a). The analogous behavior is not detected in DPPC + 20% CHOL suspension (Fig. 2b) and especially not in CHOL saturated solution (Fig. 2c) in which there is no phase transition in the examined temperature range (30 − 52 °C). We used the duel approach to extract the most significant changes occurring during heating of multilamellar DPPC (+ 20% CHOL) liposomes and CHOL saturated solution, namely differential spectral analysis and MCR-ALS method coupled with EFA (see [31,63–65] for details).

Differential spectral analysis. The differential spectral analysis (DSA) was employed to monitor the changes in the average absorbance (turbidity) of the consecutive spectra, whereby one first finds the average difference in absorbance ($\Delta A_{T+0.5}$) between two neighboring spectra, i.e.

$$\Delta A_{T+0.5} = \frac{A_{T+1} - A_T}{m}$$

where $A_{T(+1)}$ denotes the spectrum acquired at temperature T(+1) (where T goes from 30 to 51 (°C)), and m is the number of data points in spectra (in spectral range 250 − 300 nm m is 51). Afterwards, the obtained average differences in absorbance were used to build profiles presented in Fig. 2b in a cumulative fashion, following

$$A^c_{T'} = \sum_{T=30.5}^{T'} \Delta A_T$$

where $A^c_{T'}$ stands for cumulative absorbance difference. Finally, the obtained profiles were normalized in a way that $A^c_{T'}$ at 51.5 °C was set to 1, and the remaining points are determined accordingly. Overall, the procedure takes into account behavior of the spectra in the entire investigated region (250 − 300 nm) with the obtained metric ($A^c_{T'}$) being multivariate in its nature.

Multivariate curve analysis. We also applied MCR-ALS with EFA using publicly available Matlab code [66] to analyze the behavior of the systems at hand. Details of MCR-ALS with EFA procedure can be found elsewhere [63–65], whereas only the basics are outlined here. Briefly, this approach enables one to decompose data matrix **D** (temperature-dependent UV/Vis spectra in this manuscript) as the product of two matrices **C** and $\mathbf{S^T}$

$$\mathbf{D} = \mathbf{CS^T} + \mathbf{E}$$

where **C** and $\mathbf{S}^T$ refer to the concentration (**C**) and spectral ($\mathbf{S}^T$) profile of the components that exhaust the most variance from the data (in our case acquired spectra), respectively, and **E** is a matrix of residuals unexplained by the product $\mathbf{CS^T}$. In this study we employed this multivariate method by performing single-component analysis, to differ from the previous study in which two-component analysis is utilized [31]. This change, compared to the previous usage of this technique in which it is used to characterize the similar systems via temperature-dependence of FTIR spectra [31], stems from the fact that the spectra obtained in 250 − 300 nm region, when temperature-dependent UV/Vis spectroscopy is employed, are virtually linear in nature (see Fig. 2a), i.e. no significant change in the topology of the spectra appears. Thus, the first two components obtained after MCR-ALS/EFA procedure do not bear equivalent physical interpretation as previously noted [31], namely they do not correspond to the low- and high-

temperature component. Rather than that, we can now only discuss the results in purely mathematical terms, namely the single-component analysis should be thought of simply as the representation of the multidimensional data (spectral data) onto first principal component obtained after MCR-ALS/EFA procedure. In this respect, we find that the profiles obtained after single-component MCR-ALS/EFA procedure give rise to profiles bearing virtually identical signatures as the ones obtained using differential spectral analysis, implying that the first principal component (denoting the component corresponding to the largest variance of data) corresponds almost perfectly to the average difference in absorbance between the experimentally obtained spectra. Putting it differently, MCA is virtually equivalent to DSA up to the transformation in which profile is reflected over a horizontal axis. Profiles obtained from UV/Vis spectra of DPPC multilamellar liposomes, using both of the aforementioned techniques (differential spectral analysis and MCR-ALS/EFA), are sigmoidal in nature and display two inflections. The profiles were then further analyzed, whereby we determined the positions of the inflection points by performing double Boltzmann fit (R^2 values in all cases ≥ 0.992). Details on fitting parameters are presented in Supporting Information (section S1). The analogous profiles obtained from UV/Vis spectra of DPPC + 20% CHOL and CHOL are best described by a second- and first-order polynomial, with R^2 values ≥ 0.983 and 0.985, respectively.

2.3 DSC: Thermal analysis of hydrated multilamellar liposomes

DPPC and DPPC + 20% CHOL suspensions, saturated CHOL solution and reference aqueous solution(s) of NaCl (and PB) were held for 10 minutes in a degassing station before the start of the measurement. The calorimetric experiments were performed in a microcalorimeter Nano-DSC, TA Instruments (New Castle, USA) at a scan rate of 0.25 °C min^{-1}, temperature range 15 − 55 °C for reference solution(s) and 25 − 50 °C for DPPC samples in cell volume of 300 µl. Each sample was recorded twice in two heating-cooling cycles. The reference scans (of aqueous solution(s) of NaCl and PB) were collected in the same manner as samples spectra (only once) and subtracted from the raw data.

Data analysis was performed using the TA Instruments Nano Analyze software package where the baseline was manually constructed and subtracted from the resultant curve. T_p and T_m values were determined from heating-rate independent curve onsets [67] obtained by tangential method [68] as well as from the curve maxima from thermal-history free second heating run [69].

2.4 DLS measurements

The size distribution of liposomes was determined by means of dynamic light scattering using a photon correlation spectrophotometer equipped with a 532 nm (green) laser (Zetasizer Nano ZS, Malvern Instruments, Worcestershire, UK). To avoid overestimation arising from the scattering of larger particles, the average hydrodynamic diameter (d_h) was obtained as the value at peak maximum of the volume size distribution. The reported results correspond to the average of six measurements. The data processing was done by the Zetasizer software 7.13 (Malvern Instruments). d_h values of the DPPC and DPPC + 20% CHOL liposomes (at γ (DPPC / DPPC + 20% CHOL) = 0.5 mg ml^{-1}), determined by dynamic light scattering (DLS) at 25 °C, were in the range 2000 nm ≤ d_h ≤ 4000 nm for DPPC and 200 nm ≤ d_h ≤ 500 nm for DPPC + 20% CHOL and thus confirming the existence of multilamellar liposomes.

3. Results and Discussion

As NaCl aqueous solution(s) (and PB) are completely transparent in UV/Vis region, their temperature-dependent spectra are more or less straight horizontal lines (see Supporting Information, Fig. S2). In DPPC suspensions the inherent turbidity of the suspensions causes a background signal uplift and represents the signature of multilamellar liposomes in the UV/Vis region (Fig. 2a). Since the turbidity of solutions changes with temperature (the solution becomes more transparent with increasing temperature), the change in the background signal absorbance with temperature is a function of temperature-dependent behavior of lipid molecules in multilamellar liposomes. (More details on the formalism that links macroscopic and molecular properties of lipid suspensions are presented in [70–72].)

When normalized cumulative absorbance difference and the difference in the spectra along the first principal component (see subsection 2.2) are presented as a function of temperature, the curves with the double sigmoidal character are observed (Fig. 2d). Furthermore, the inflection points of the curves coincide with T_p (~ 33 − 34 °C) and T_m (~ 40 − 42 °C) of DPPC [3]. Their precise values, presented in Table 1, suggest that, effectively, there is no differences between the results obtained by these two approaches.

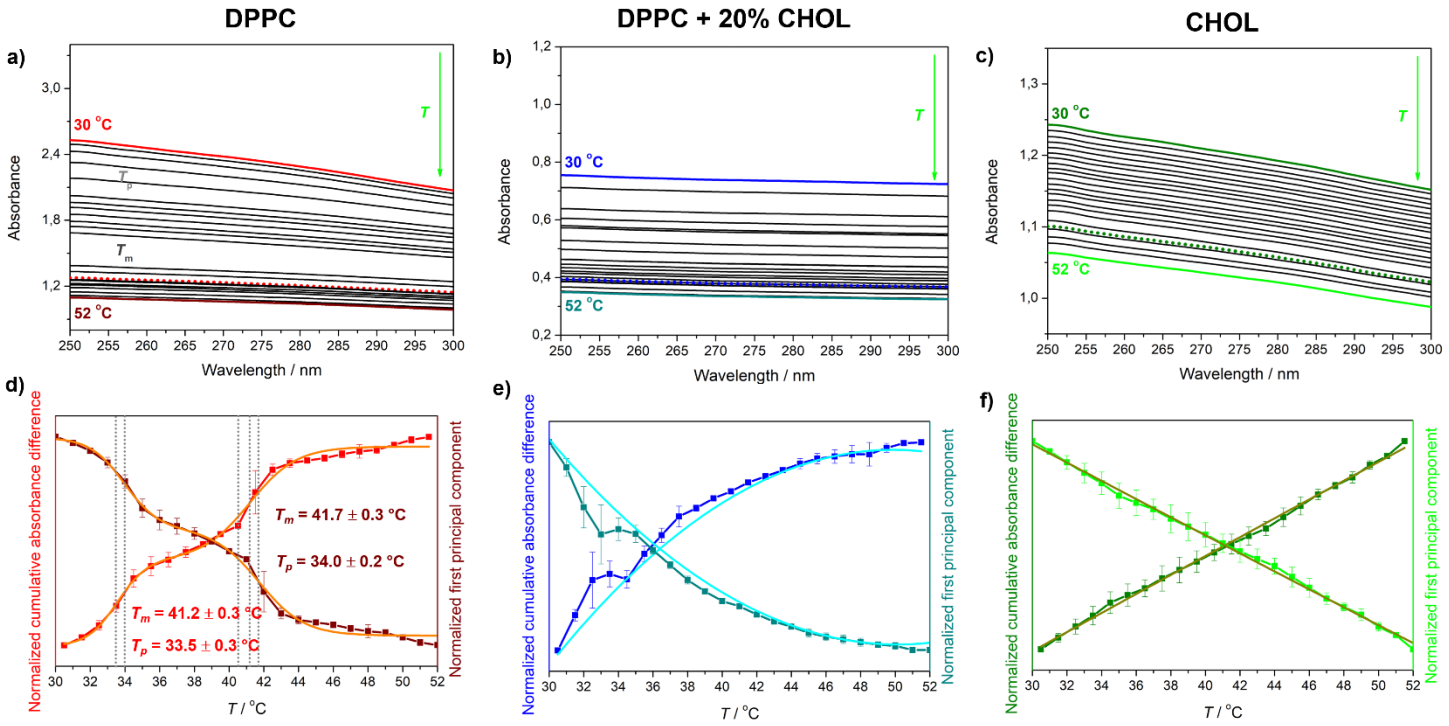

Fig. 2. Temperature-dependent UV/Vis spectra of with the lowest (30 °C) and the highest temperature (52 °C) highlighted along with the spectral profile obtained from MCA (dotted line): a) DPPC in NaCl (I = 100 mM); b) DPPC + 20% CHOL in NaCl (I = 100 mM); c) CHOL in NaCl (I = 100 mM)). The discontinuities in sample turbidity/absorbance values in DPPC suspension (a) coincides with T_p and T_m; Normalized cumulative absorbance difference (DSA) and spectra projected onto the normalized first principal component (MCA) as a function of temperature: d) DPPC in NaCl (I = 100 mM) designated with red and wine lines and double sigmoidal fit with orange line (T_p and T_m (dotted vertical gray lines) are labeled with corresponding colors); e) DPPC + 20 % CHOL in NaCl (I = 100 mM) designated with blue and darky cyan lines and double sigmoidal fit with cyan line; f) CHOL in NaCl (I = 400 mM) designated with olive and green lines and double sigmoidal fit with dark yellow line.

Concerning DSC measurements (Fig. 3a), at the applied heating rate (1 °C min^{-1}) the pretransition is resolved from the main phase transition for DPPC suspension and the corresponding temperatures of DPPC suspension are, determined from the onset/maximum, T_p = 33.4 ± 0.2 °C / 36.4 ± 0.1 °C and T_m = 40.8 ± 0.1 °C / 41.9 ± 0.1 °C (Table 1). (Analogous quantities of DPPC suspended in other two hydrating media, along with associated explanation, are presented in Supporting Information, section S3).

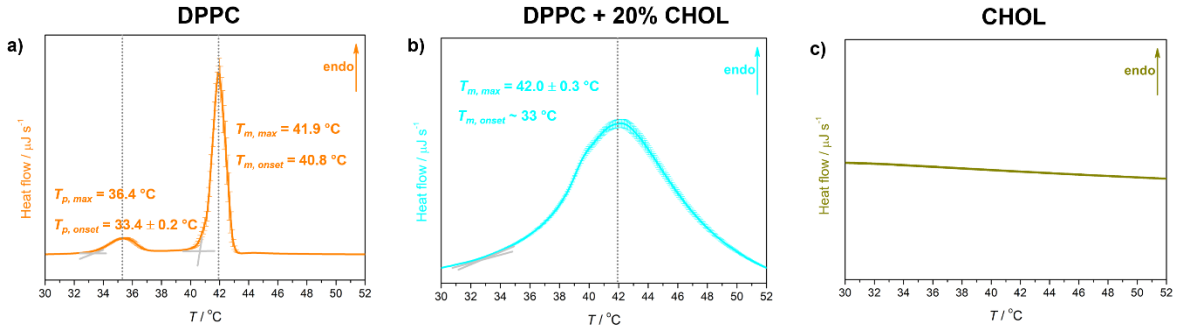

Fig. 3. DSC curves obtained at heating rate of 1 °C min^{-1} for: a) DPPC in NaCl (I = 100 mM) designated with orange line (T_p and T_m are determined from both onset and curve maxima, respectively, and are labeled with corresponding colors); b) DPPC + 20% CHOL in NaCl (I = 100 mM) designated with cyan line (T_m is determined from both onset and curve maxima, respectively); c) CHOL in NaCl (I = 100 mM) designated with dark yellow line.

The absence of sigmoidal character in the profiles obtained from UV/Vis spectra of DPPC + CHOL mixtures (Fig. 2b and 2e) suggest that the observed phase transition is most likely not overly related to the cooperative behavior between DPPC molecules. This is supported by the data we obtained from DSC profile of this mixture; it consists of one broad signal with T_m ~ 33 ° C determined from the onset and T_m = 42.0 ± 0.3 °C determined from the curve maximum (see Fig. 3b and Table 1). According to the literature, this broad component could be attributed either to the transition between L_o (liquid-ordered) and L_d (liquid disordered) phases [73,74] or to the melting of condensed complexes [75]. A small irregularity, partly hidden due to the error bars, at about 40 °C (labelled as * in Fig. 3b) reflects the melting of almost pure DPPC regions [76]. Moreover, the full width at half maximum (FWHM), which is a parameter correlated with phase transition cooperativity [77], of this single thermotropic event in DPPC + CHOL mixture is FWHM ≈ 8 °C and is considerably higher than corresponding values of two separate thermotropic events in pure DPPC with FWHMs being FWHM ≈ 2.5 °C and FWHM ≈ 1 °C, for pre- and main phase transition, respectively.

Only linear profiles observed for CHOL in NaCl suspension originate from the temperature-dependent behavior of saturated CHOL solution in which, in the examined temperature range, there is no thermotropic event (Fig. 2c, 2f, 3c).

Table 1. Phase transitions temperatures (T_{pt}) of DPPC and DPPC + 20% CHOL mixtures (and saturated CHOL solutions) suspended in aqueous solution (I(NaCl) = 100 mM) determined from DSC curves (by reading the transition onset and maximum) and temperature-dependent UV/Vis spectra analyzed using DSA and MCA

System	T_{pt}[a]					
	DSC[b]		UV/Vis			
			DSA		MCA	
	T_p	T_m	T_p	T_m	T_p	T_m
DPPC	33.4 ± 0.2 (onset) 36.4 (max)	40.8 (onset) 41.9 (max)	33.5 ± 0.3	41.2 ± 0.3	34.0 ± 0.2	41.7 ± 0.3
DPPC + 20% CHOL	–	~ 33 (onset) 42.0 ± 0.3 (max)	–	–	–	–
CHOL	–	–	–	–	–	–

[a] In °C; [b] When not designated explicitly, uncertainty associated with T_m values determined from DSC curves is ± 0.1 °C.

When we compare the results obtained by UV/Vis spectroscopy and via DSC we come to two important conclusions related to DPPC: i) the temperature of the main phase transition (T_m) determined from DSC measurements, whether obtained by reading onset or the maximum of the corresponding transition, shows excellent agreement with the temperatures determined from temperature-dependent UV/Vis spectra, regardless of the approach used in data analysis. This (first) conclusion essentially presents nothing extraordinary and actually confirms the findings reported by Cevc *et al*. [55] obtained in univariate fashion; ii) the low-cooperativity pretransition at the applied heating rate (1 °C min^{-1}) is of much lower intensity than high-cooperativity main phase transition observable from DSC curve (it would be easy to overlook it if it was not expected in exactly that temperature range). This is definitely not unexpected since the heating rate is one of the most important factors influencing the intensity of thermotropic events during calorimetric measurements [77]. What is truly surprising is the ability to detect the same transition under the same measurement conditions from temperature-dependent UV/Vis spectra. Moreover, the pretransition is, according to the difference between the plateaus of the obtained curves (Fig. 2d), as easily detectible as the main phase transition (for more details see Supporting Information, Fig. S1 and Table S1). If, however, the thermotropic event under exploration is related with compositional heterogeneities such as in DPPC + 20% CHOL mixture [76], multivariate analyses of their UV/Vis spectra will generate non-sigmoidal profiles (second-order polynomial), suggesting the absence of cooperative lipid behavior as seen in single-lipid component liposomes. In suspensions without thermotropic events (CHOL) only linear profiles are to be expected, similarly to the profiles generated by water combination band observed in FTIR spectra of DPPC and DPPE suspensions [31]. The pretransition-related findings associated with a single lipid species give rise to a two-faceted phenomenon − the data obtained from temperature-dependent UV/Vis spectra, in terms of the differences between the plateaus of two discontinuities, do not reflect the cooperativity degree of the detected phase transition (in comparison with other phase transitions observed in explored temperature range). This is, for instance, not the case with FTIR data in which the magnitude of the plateaus differences can be correlated with the cooperativity degree of the encompassed phase transition [31]. Overall, this suggest that UV/Vis spectral data are invariant on the phase transition cooperativity degree. However, from the other side of the same phenomenon an outstanding advantage emerges: temperature-dependent UV/Vis spectroscopy might just be powerful and potent enough in this respect to enable detection of phase transitions so weak that they have not been possible to capture by conventional thermoanalytical techniques thus far.

4. Conclusion

To date, knowledge of the cooperativity degree of individual lipid phase transitions has relied primarily on data obtained from DSC measurements. Since these data are a function of operating conditions, there is a certain possibility that individual phase transitions of (extremely) low-cooperativity will go unnoticed. The conducted study clearly indicates that by multivariate analyses of temperature-dependent UV/Vis spectra one can detect not just all lipid phase transitions in the explored range, but also that low-cooperativity phase transitions can be registered with the same sensitivity as those of high-cooperativity. Accordingly, we believe that this approach could be applied in the study of more dilute solutions on an instrument of equal sensitivity, while the study on instruments of lower sensitivity should be conducted in cuvettes of greater path length or higher sample concentration. This remarkable finding paves new pathways not only in the detection and identification of lipid phase transitions that may have gone unnoticed so far, but also in any possible structural changes in the organization of lipid bilayers resulting in minimal changes in suspension turbidity. In this respect further investigations focused on both individual lipids as well as on lipid mixtures are underway.

Supporting Information

Supporting Information associated with this paper can be found in the online version at http://.

Acknowledgment

This paper was supported by Croatian Science Foundation, Project No. UIP-2020-02-7669. P. M. and D. B. gratefully acknowledge Dr. Ivo Crnolatac (Laboratory for Biomolecular Interactions and Spectroscopy, Ruđer Bošković Institute) for technical assistance in performing UV/Vis measurements.

References:

[1] L. Farine, M. Niemann, A. Schneider, P. Bütikofer, Phosphatidylethanolamine and phosphatidylcholine biosynthesis by the Kennedy pathway occurs at different sites in Trypanosoma brucei, Sci. Rep. 5 (2015) 1–11. https://doi.org/10.1038/srep16787.

[2] J.N. van der Veen, J.P. Kennelly, S. Wan, J.E. Vance, D.E. Vance, R.L. Jacobs, The critical role of phosphatidylcholine and phosphatidylethanolamine metabolism in health and disease, Biochim. Biophys. Acta - Biomembr. 1859 (2017) 1558–1572. https://doi.org/10.1016/j.bbamem.2017.04.006.

[3] R. Koynova, M. Caffrey, Phases and phase transitions of the phosphatidylcholines, Biochim. Biophys. Acta. 1376 (1998) 91–145. https://doi.org/10.1016/S0013-4686(03)00208-1.

[4] W. Shinoda, Permeability across lipid membranes, Biochim. Biophys. Acta - Biomembr. 1858 (2016) 2254–2265. https://doi.org/10.1016/j.bbamem.2016.03.032.

[5] B. Qiao, M. Olvera De La Cruz, Driving force for water permeation across lipid membranes, J. Phys. Chem. Lett. 4 (2013) 3233–3237. https://doi.org/10.1021/jz401730s.

[6] R.M. Cordeiro, Molecular Structure and Permeability at the Interface between Phase-Separated Membrane Domains, J. Phys. Chem. B. 122 (2018) 6954–6965. https://doi.org/10.1021/acs.jpcb.8b03406.

[7] A. Blicher, K. Wodzinska, M. Fidorra, M. Winterhalter, T. Heimburg, The temperature dependence of lipid membrane permeability, its quantized nature, and the influence of anesthetics, Biophys. J. 96 (2009) 4581–4591. https://doi.org/10.1016/j.bpj.2009.01.062.

[8] M. Jansen, A. Blume, A comparative study of diffusive and osmotic water permeation across bilayers composed of phospholipids with different head groups and fatty acyl chains, Biophys. J. 68 (1995) 997–1008. https://doi.org/10.1016/S0006-3495(95)80275-4.

[9] S. Paula, A.G. Volkov, A.N. Van Hoek, T.H. Haines, D.W. Deamer, Permeation of protons, potassium ions, and small polar molecules through phospholipid bilayers as a function of membrane thickness, Biophys. J. 70 (1996) 339–348. https://doi.org/10.1016/S0006-3495(96)79575-9.

[10] J.C. Mathai, S. Tristram-Nagle, J.F. Nagle, M.L. Zeidel, Structural determinants of water permeability through the lipid membrane, J. Gen. Physiol. 131 (2008) 69–76. https://doi.org/10.1085/jgp.200709848.

[11] M.T. Montero, J. Hernàndez-Borrell, K.M.W. Keough, Fluoroquinolone-biomembrane interactions: Monolayer and calorimetric studies, Langmuir. 14 (1998) 2451–2454. https://doi.org/10.1021/la9706882.

[12] M. Arczewska, D.M. Kamiński, E. Górecka, D. Pociecha, E. Rój, A. Sławińska-Brych,

M. Gagoś, The molecular organization of prenylated flavonoid xanthohumol in DPPC multibilayers: X-ray diffraction and FTIR spectroscopic studies, Biochim. Biophys. Acta - Biomembr. 1828 (2013) 213–222. https://doi.org/10.1016/j.bbamem.2012.10.009.

[13] A. Kenaan, J. Cheng, D. Qi, D. Chen, D. Cui, J. Song, Physicochemical Analysis of DPPC and Photopolymerizable Liposomal Binary Mixture for Spatiotemporal Drug Release, Anal. Chem. 90 (2018) 9487–9494. https://doi.org/10.1021/acs.analchem.8b02144.

[14] S.K. Tsermentseli, K.N. Kontogiannopoulos, V.P. Papageorgiou, A.N. Assimopoulou, Comparative study of PEGylated and conventional liposomes as carriers for shikonin, Fluids. 3 (2018) 1–16. https://doi.org/10.3390/fluids3020036.

[15] H. Bensikaddour, K. Snoussi, L. Lins, F. Van Bambeke, P.M. Tulkens, R. Brasseur, E. Goormaghtigh, M.P. Mingeot-Leclercq, Interactions of ciprofloxacin with DPPC and DPPG: Fluorescence anisotropy, ATR-FTIR and ^{31}P NMR spectroscopies and conformational analysis, Biochim. Biophys. Acta - Biomembr. 1778 (2008) 2535–2543. https://doi.org/10.1016/j.bbamem.2008.08.015.

[16] H. Bensikaddour, N. Fa, I. Burton, M. Deleu, L. Lins, A. Schanck, R. Brasseur, Y.F. Dufrêne, E. Goormaghtigh, M.P. Mingeot-Leclercq, Characterization of the interactions between fluoroquinolone antibiotics and lipids: A multitechnique approach, Biophys. J. 94 (2008) 3035–3046. https://doi.org/10.1529/biophysj.107.114843.

[17] A. Sadžak, Z. Brkljača, I. Crnolatac, G. Baranović, S. Šegota, Flavonol clustering in model lipid membranes: DSC, AFM, force spectroscopy and MD simulations study, Colloids Surfaces B Biointerfaces. 193 (2020) 111147. https://doi.org/10.1016/j.colsurfb.2020.111147.

[18] K. Cieślik-Boczula, J. Szwed, A. Jaszczyszyn, K. Gasiorowski, A. Koll, Interactions of dihydrochloride fluphenazine with DPPC liposomes: ATR-IR and ^{31}P NMR studies, J. Phys. Chem. B. 113 (2009) 15495–15502. https://doi.org/10.1021/jp904805t.

[19] S.E. Schullery, T.A. Seder, D.A. Weinstein, D.A. Bryant, Differential Thermal Analysis of Dipalmitoylphosphatidylcholine-Fatty Acid Mixturest, (1981) 6818–6824.

[20] J.F. Nagle, P. Cognet, F.G. Dupuy, S. Tristram-Nagle, Structure of gel phase DPPC determined by X-ray diffraction, Chem. Phys. Lipids. 218 (2019) 168–177. https://doi.org/10.1016/j.chemphyslip.2018.12.011.

[21] K. Akabori, J.F. Nagle, Structure of the DMPC lipid bilayer ripple phase, Soft Matter. 11 (2015) 918–926. https://doi.org/10.1039/c4sm02335h.

[22] B.A. Cunningham, A.D. Brown, D.H. Wolfe, W.P. Williams, A. Brain, Ripple phase formation in phosphatidylcholine: Effect of acyl chain relative length, position, and unsaturation, Phys. Rev. E - Stat. Physics, Plasmas, Fluids, Relat. Interdiscip. Top. 58 (1998) 3662–3672. https://doi.org/10.1103/PhysRevE.58.3662.

[23] M.P. Hentschel, F. Rustichelli, Structure of the Ripple Phase P in Hydrated Phosphatidylcholine Multimembranes, Phys. Rev. Lett. 66 (1991) 903–906. https://doi.org/10.1103/PhysRevLett.66.903.

[24] G. Pabst, M. Rappolt, H. Amenitsch, P. Laggner, Structural information from multilamellar liposomes at full hydration: Full q-range fitting with high quality X-ray data, Phys. Rev. E - Stat. Physics, Plasmas, Fluids, Relat. Interdiscip. Top. 62 (2000) 4000–4009. https://doi.org/10.1103/PhysRevE.62.4000.

[25] M. Rappolt, G. Pabst, G. Rapp, M. Kriechbaum, H. Amenitsch, C. Krenn, S. Bernstorff, P. Laggner, New evidence for gel-liquid crystalline phase coexistence in the ripple phase of phosphatidylcholines, Eur. Biophys. J. 29 (2000) 125–133. https://doi.org/10.1007/s002490050257.

[26] K. Sengupta, V.A. Raghunathan, J. Katsaras, Novel structural features of the ripple phase of phospholipids, Europhys. Lett. 49 (2000) 722–728. https://doi.org/10.1209/epl/i2000-00210-x.

[27] K. Sengupta, V.A. Raghunathan, Y. Hatwalne, Role of tilt order in the asymmetric ripple phase of phospholipid bilayers, Phys. Rev. Lett. 87 (2001) 55705-1-55705–4. https://doi.org/10.1103/PhysRevLett.87.055705.

[28] W.-J. Sun, S. Tristram-Nagle, R.M. Suter, J.F. Nagle, Structure of the ripple phase in lecithin bilayers, Proc. Natl. Acad. Sci. U. S. A. 93 (1996) 7008–7012.

[29] D.C. Wack, W.W. Webb, Synchrotron x-ray study of the modulated lamellar phase Pbeta' in the lecithin-water system, Phys. Rev. A. 40 (1989) 2712–2730.

[30] T. Kaasgaard, C. Leidy, J.H. Crowe, O.G. Mouritsen, K. Jørgensen, Temperature-controlled structure and kinetics of ripple phases in one- and two-component supported lipid bilayers, Biophys. J. 85 (2003) 350–360. https://doi.org/10.1016/S0006-

3495(03)74479-8.

[31] P. Maleš, Z. Brkljača, I. Crnolatac, D. Bakarić, Application of MCR-ALS with EFA on FT-IR spectra of lipid bilayers in the assessment of phase transition temperatures: Potential for discernment of coupled events, Colloids Surfaces B Biointerfaces. 201 (2021). https://doi.org/10.1016/j.colsurfb.2021.111645.

[32] H.L. Casal, H.H. Mantsch, The thermotropic phase behavior of *N*-methylated dipalmitoylphosphatidylethanolamines, BBA - Biomembr. 735 (1983) 387–396. https://doi.org/10.1016/0005-2736(83)90153-0.

[33] D.G. Cameron, H.L. Casal, H.H. Mantsch, Characterization of the Pretransition in 1, 2-Dipalmitoyl-Sn-Glycero-3-Phosphocholine by Fourier Transform Infrared Spectroscopy, Biochemistry. 19 (1980) 3665–3672. https://doi.org/10.1021/bi00557a005.

[34] T. Le Bihan, M. Pézolet, Study of the structure and phase behavior of dipalmitoylphosphatidylcholine by infrared spectroscopy: Characterization of the pretransition and subtransition, Chem. Phys. Lipids. 94 (1998) 13–33. https://doi.org/10.1016/S0009-3084(98)00022-X.

[35] R.O. Seitter, T. Link, R. Kimmich, A. Kobelkov, P. Wolfangel, K. Müller, Deuteron spectroscopy and deuteron field-cycling nuclear magnetic resonance relaxometry of the hydration water of lipid bilayers: The corrugated-sheet model for interface molecular dynamics in the ripple phase, J. Chem. Phys. 112 (2000) 8715–8722. https://doi.org/10.1063/1.481473.

[36] T. Sparrman, P.O. Westlund, An NMR line shape and relaxation analysis of heavy water powder spectra of the L_{α}, $L_{\beta'}$ and $P_{\beta'}$ phases in the DPPC/water system, Phys. Chem. Chem. Phys. 5 (2003) 2114–2121. https://doi.org/10.1039/b211471b.

[37] A.H. De Vries, S. Yefimov, A.E. Mark, S.J. Marrink, Molecular structure of the lecithin ripple phase, Proc. Natl. Acad. Sci. U. S. A. 102 (2005) 5392–5396. https://doi.org/10.1073/pnas.0408249102.

[38] S. Leekumjorn, A.K. Sum, Molecular simulation study of structural and dynamic properties of mixed DPPC/DPPE bilayers, Biophys. J. 90 (2006) 3951–3965. https://doi.org/10.1529/biophysj.105.076596.

[39] S. Leekumjorn, A.K. Sum, Molecular studies of the gel to liquid-crystalline phase transition for fully hydrated DPPC and DPPE bilayers, Biochim. Biophys. Acta - Biomembr. 1768 (2007) 354–365. https://doi.org/10.1016/j.bbamem.2006.11.003.

[40] O. Lenz, F. Schmid, Structure of symmetric and asymmetric "ripple" phases in lipid bilayers, Phys. Rev. Lett. 98 (2007) 2–5. https://doi.org/10.1103/PhysRevLett.98.058104.

[41] P. Khakbaz, J.B. Klauda, Investigation of phase transitions of saturated phosphocholine lipid bilayers via molecular dynamics simulations, Biochim. Biophys. Acta - Biomembr. 1860 (2018) 1489–1501. https://doi.org/10.1016/j.bbamem.2018.04.014.

[42] T. Heimburg, Thermal Biophysics of Membranes, Wiley-VCH, Weinheim, 2007.

[43] T. Heimburg, A model for the lipid pretransition: Coupling of ripple formation with the chain-melting transition, Biophys. J. 78 (2000) 1154–1165. https://doi.org/10.1016/S0006-3495(00)76673-2.

[44] B.G. Tenchov, H. Yao, I. Hatta, Time-resolved x-ray diffraction and calorimetric studies at low scan rates: I. Fully hydrated dipalmitoylphosphatidylcholine (DPPC) and DPPC/water/ethanol phases, Biophys. J. 56 (1989) 757–768. https://doi.org/10.1016/S0006-3495(89)82723-7.

[45] K.A. Riske, R.P. Barroso, C.C. Vequi-Suplicy, R. Germano, V.B. Henriques, M.T. Lamy, Lipid bilayer pre-transition as the beginning of the melting process, Biochim. Biophys. Acta - Biomembr. 1788 (2009) 954–963. https://doi.org/10.1016/j.bbamem.2009.01.007.

[46] R. Zimmermann, D. Küttner, L. Renner, M. Kaufmann, C. Werner, Fluidity modulation of phospholipid bilayers by electrolyte ions: Insights from fluorescence microscopy and microslit electrokinetic experiments, J. Phys. Chem. A. 116 (2012) 6519–6525. https://doi.org/10.1021/jp212364q.

[47] D. Bakarić, D. Petrov, Y. Kunhi Mouvenchery, S. Heissler, C. OOstenbrink, G.E. Schaumann, Ion-induced modification of the sucrose network and its impact on melting of freeze-dried liposomes. DSC and molecular dynamics study, Chem. Phys. Lipids. 210 (2018) 38–46.

[48] H.I. Petrache, S. Tristram-Nagle, D. Harries, N. Kučerka, J.F. Nagle, V.A. Parsegian,

Swelling of phospholipids by monovalent salt, J. Lipid Res. 47 (2006) 302–309. https://doi.org/10.1194/jlr.M500401-JLR200.

[49] P. Beaumont, A. Courtois, T. Richard, S. Krisa, C. Faure, Encapsulation of ε-viniferin into multi-lamellar liposomes: Development of a rapid, easy and cost-efficient separation method to determine the encapsulation efficiency, Pharmaceutics. 13 (2021) NA. https://doi.org/10.3390/pharmaceutics13040566.

[50] D. Xu, J. Xie, X. Feng, X. Zhang, Z. Ren, Y. Zheng, J. Yang, Preparation and evaluation of a Rubropunctatin-loaded liposome anticancer drug carrier, RSC Adv. 10 (2020) 10352–10360. https://doi.org/10.1039/c9ra10390b.

[51] P. Panwaer, B. Pandey, P.C. Lakhera, K.P. Singh, Preparation, characterization, and in vitro release study of albendazole-encapsulated nanosize liposomes, Int. J. Nanomedicine. 5 (2010) 101–108.

[52] S. Krishna Prasad, R. Shashidhar, B.P. Gaber, S.C. Chandrasekhar, Pressure studies on two hydrated phospholipids - 1,2-dimyristoyl-phosphatidylcholine and 1,2-dipalmitoyl-phosphatidylcholine, Chem. Phys. Lipids. 43 (1987) 227–235. https://doi.org/10.1016/0009-3084(87)90010-7.

[53] E.S. Rowe, Lipid Chain Length and Temperature Dependence of Ethanol-Phosphatidylcholine Interactions, Biochemistry. 22 (1983) 3299–3305.

[54] S. Kaneshina, H. Ichimori, T. Hata, H. Matsuki, Barotropic phase transitions of dioleoylphosphatidylcholine and stearoyl-oleoylphosphatidylcholine bilayer membranes, Biochim. Biophys. Acta - Biomembr. 1374 (1998) 1–8. https://doi.org/10.1016/S0005-2736(98)00122-9.

[55] G. Cevc, J.M. Seddon, R. Hartung, W. Eggert, Phosphatidylcholine-fatty acid membranes. I. Effects of protonation, salt concentration, temperature and chain-length on the colloidal and phase properties of mixed vesicles, bilayers and nonlamellar structures, BBA - Biomembr. 940 (1988) 219–240. https://doi.org/10.1016/0005-2736(88)90197-6.

[56] D.A. Mannock, R.N.A.H. Lewis, R.N. McElhaney, Comparative calorimetric and spectroscopic studies of the effects of lanosterol and cholesterol on the thermotropic phase behavior and organization of dipalmitoylphosphatidylcholine bilayer membranes, Biophys. J. 91 (2006) 3327–3340. https://doi.org/10.1529/biophysj.106.084368.

[57] M.G.K. Benesch, D.A. Mannock, R.N. McElhaney, Sterol chemical configuration influences the thermotropic phase behaviour of dipalmitoylphosphatidylcholine bilayers containing 5α-cholestan- 3β- and 3α-ol, Chem. Phys. Lipids. 164 (2011) 70–77. https://doi.org/10.1016/j.chemphyslip.2010.10.003.

[58] S. Šegota, D. Vojta, G. Pletikapić, G. Baranović, Ionic strength and composition govern the elasticity of biological membranes. A study of model DMPC bilayers by force- and transmission IR spectroscopy, Chem. Phys. Lipids. 186 (2015) 17–29. https://doi.org/10.1016/j.chemphyslip.2014.11.001.

[59] S. Garcia-Manyes, G. Oncins, F. Sanz, Effect of ion-binding and chemical phospholipid structure on the nanomechanics of lipid bilayers studied by force spectroscopy, Biophys. J. 89 (2005) 1812–1826. https://doi.org/10.1529/biophysj.105.064030.

[60] S. Garcia-Manyes, G. Oncins, F. Sanz, Effect of temperature on the nanomechanics of lipid bilayers studied by force spectroscopy, Biophys. J. 89 (2005) 4261–4274. https://doi.org/10.1529/biophysj.105.065581.

[61] M. Leitgeb, Ž. Knez, M. Primožič, Sustainable technologies for liposome preparation, J. Supercrit. Fluids. 165 (2020) 104984.

[62] F. Menges, Spectragryph, "Spectragryph - optical spectroscopy software", Version 1.2.15, 2015, http://www.effemm2.de/spectragryph/, (15.12.2021).

[63] A. De Juan, J. Jaumot, R. Tauler, Multivariate Curve Resolution (MCR). Solving the mixture analysis problem, Anal. Methods. 6 (2014) 4964–4976. https://doi.org/10.1039/c4ay00571f.

[64] M. Maeder, A. de Juan, Two-Way Data Analysis: Evolving Factor Analysis, Compr. Chemom. 2 (2009) 261–274. https://doi.org/10.1016/B978-044452701-1.00047-8.

[65] H.R. Keller, D.L. Massart, Evolving factor analysis, Chemom. Intell. Lab. Syst. 12 (1991) 209–224. https://doi.org/10.1016/0169-7439(92)80002-L.

[66] J. Jaumot, R. Gargallo, A. De Juan, R. Tauler, A graphical user-friendly interface for MCR-ALS: A new tool for multivariate curve resolution in MATLAB, Chemom. Intell. Lab. Syst. 76 (2005) 101–110. https://doi.org/10.1016/j.chemolab.2004.12.007.

[67] G.W.H. Hohne, H.K. Cammenga, W. Eysel, E. Gmelin, W. Hemminger, THE TEMPERATURE CALIBRATION OF SCANNING CALORIMETERS G.W.H.,

Thermochim. Acta. 160 (1990) 1–12.

[68] R. Maddalena, H. Taha, D. Gardner, Self-healing potential of supplementary cementitious materials in cement mortars: Sorptivity and pore structure, Dev. Built Environ. 6 (2021) 100044. https://doi.org/10.1016/j.dibe.2021.100044.

[69] C. Chen, D. Han, C. Cai, X. Tang, An overview of liposome lyophilization and its future potential, J. Control. Release. 142 (2010) 299–311. https://doi.org/10.1016/j.jconrel.2009.10.024.

[70] T.G. Mayerhöfer, A. Dabrowska, A. Schwaighofer, B. Lendl, J. Popp, Beyond Beer's Law: Why the Index of Refraction Depends (Almost) Linearly on Concentration, ChemPhysChem. 21 (2020) 707–711. https://doi.org/10.1002/cphc.202000018.

[71] T.G. Mayerhöfer, J. Popp, Beer's Law – Why Absorbance Depends (Almost) Linearly on Concentration, ChemPhysChem. 20 (2019) 511–515. https://doi.org/10.1002/cphc.201801073.

[72] T.G. Mayerhöfer, J. Popp, Beyond Beer's Law: Revisiting the Lorentz-Lorenz Equation, ChemPhysChem. 21 (2020) 1218–1223. https://doi.org/10.1002/cphc.202000301.

[73] J. Hjort Ipsen, G. Karlström, O.G. Mourtisen, H. Wennerström, M.J. Zuckermann, Phase equilibria in the phosphatidylcholine-cholesterol system, BBA - Biomembr. 905 (1987) 162–172. https://doi.org/10.1016/0005-2736(87)90020-4.

[74] K. Simons, W.L.C. Vaz, Model systems, lipid rafts, and cell membranes, Annu. Rev. Biophys. Biomol. Struct. 33 (2004) 269–295. https://doi.org/10.1146/annurev.biophys.32.110601.141803.

[75] T.G. Anderson, H.M. Mcconnell, Condensed Complexes and the Calorimetry of Cholesterol-Phospholipid Bilayers, Biophys. J. 81 (2001) 2774–2785.

[76] P.F. Almeida, F.E. Carter, K.M. Kilgour, M.H. Raymonda, E. Tejada, Heat Capacity of DPPC/Cholesterol Mixtures: Comparison of Single Bilayers with Multibilayers and Simulations, Langmuir. 34 (2018) 9798–9809. https://doi.org/10.1021/acs.langmuir.8b01774.

[77] R.N.A.H. Lewis, D.A. Mannock, R.N. McElhaney, Differential Scanning Calorimetry in the Study of Lipid Phase Transitions in Model and Biological Membranes, in: A.M. Dopico (Ed.), Methods Membr. Lipids, Humana Press, New Jersey, 2006: pp. 171–195.